Electronic Supplementary Material (ESI) for ChemComm.

A high dimensional oxysulfide built from large Iron-based clusters with partial charge-ordering

SUPPLEMENTARY INFORMATION

S1. Experimental Methods

Synthesis: Single crystals of $Ba_{10}Fe_{7.75}Zn_{5.25}S_{18}Si_3O_{12}$ were initially found throughout a synthesis strategy aiming at forming original compounds with heteroleptic Fe-based oxysulfide units. We attempted to synthesize a single-phase material from a stoichiometric mixture of the precursors BaO/Fe/ZnO/Zn/Si/S. Those precursors were mixed and thoroughly ground in an agate mortar before being pressed into pellets and heated in an evacuated sealed quartz tube. The heat treatment consisted in heating up to 500°C at a rate of about 30°C/h for 5 hours, then cooling down to room temperature at a 50°C/h rate. Then a second treatment was applied to the obtained powder: it was thoroughly ground in an agate mortar before being pressed into pellets, heated up to 500°C at a rate of about 30°C/h for 5 hours, then to 750°C in 8 hours for 24 hours then cooling down to 650°C at a 10°C/h rate, temperature at which the furnace was switched off.

Single crystal X-ray diffraction was performed on an X8 diffractometer equipped with a bi-dimensional CCD 4K detector and an Ag K_α source.

Powder X-ray diffraction pattern was collected on a Bruker D8 diffractometer equipped with a linear detector Lynxeye ($Cu_{K\alpha}$) in Bragg-Brentano geometry at room temperature.

Scanning electron microscopy (SEM) SEM and energy dispersive X-ray spectrum (EDS) analysis were performed on monocrystals placed on a carbon tape and graphited to avoid surfaces charging. Samples were introduced in a field-emission gun SEM HITACHI S4700 device equipped with and EDS detector, operating at 20 kV electron beam energy.

Resistivity measurements: The resistivity vs temperature curve was measured under applied DC magnetic field of 1000 Oe and at temperatures in the range of 150–350 K using a four-probe method on a Physical Property Measurement System (PPMS) Dynacool 9T from Quantum Design.

Magnetic measurements (*DC* and *AC*): The magnetic properties were measured on the same PPMS. Magnetic measurements were perform using a grinded polycrystalline sample. Typical measurements were performed using zero field cooling (ZFC) and field cooling (FC) procedures under 1000 oe. Magnetization *against field loops* were measured between −9 and 9 T at various temperatures. AC magnetic susceptibility measurements were carried out on 29 mg of sample loaded into a polycarbonate capsule, attached to the sample rod, and lowered into the cryostat of the PPMS. The in-phase and the out-of-phase components of the AC susceptibility were recorded over the temperature range from 2 K to 7 K upon heating at different frequencies between 500 Hz and 30 kHz. For all measurements the amplitude of the applied alternating magnetic field was 16 Oe.

X-ray photoelectron spectroscopy (XPS) experiments were performed using an AXIS Ultra DLD Kratos spectrometer equipped with a monochromatized aluminum source (Al K_α= 1486.6 eV). The Kratos charge neutralizer system was used during all analysis. All Binding Energies (BE) were referenced to the carbon peak corresponding to C-C bonding in the C 1s core level at 284.8 eV. Simulation of the experimental photopeaks was carried out using a mixed Gaussian(70%)/Lorentzian(30%) peak fit procedure according to the software supplied by CasaXPS. Semiquantitative analysis accounted for a nonlinear Shirley type background subtraction.

Table S1. Data Collection and Refinement Details from the single crystal XRD refinement

Formula	$Ba_{10}Fe_{7.75}Zn_{5.25}S_{18}Si_3O_{12}$
Molecular weight (g. mol^{-1})	3002.7
Symmetry	*cubic*
Space group	I -4 3 m (217)
Unit cell dimensions (Å)	a=13.33800(10)
Volume ($Å^3$)	2372.86(3)
Z	2
Data Collection	
Equipment	Bruker CCD
Λ [Ag K_α; Å]	0.56087
Temperature (K)	293
Calculated density (g cm^{-3})	2.1013
Crystal dimension (μm)	70×50×10
Color	Black
Absorption correction	analytical
Scan mode	ω, ϕ
θ (min−max) (°)	1.7-21.87
μ (mm−1 ; for λ Kα = 0.56087Å)	3.652
F(000)	2690
Reciprocal space recording	−16 ≤ h ≤ 17 −17 ≤ k ≤ 17 −17 ≤ l ≤ 17
No. of measured reflections	33587
No. of independent reflections	586
I > 3σ(I) (total)	517
Refinement	
Number of refined parameters	30
Refinement method	Least-squares
Weighting scheme	sigma
R1(F) [I > 3σ(I)]/R1(F^2) (all data, %)	0.0223/0.0291
wR2(F^2) [I > 3σ(I)]/wR2(F^2) (all data, %)	0.0246/ 0.0275
Goodness of Fit	1.31
Max/Min residual electronic density ($e^-/Å^3$)	1.50/ -0.88
Tmin/Tmax	0.8727/1.000
Flack parameter	0.04(8)

Table S2. Atomic Positions and Isotropic Thermal Displacement for $Ba_{10}Fe_{7.75}Zn_{5.25}S_{18}Si_3O_{12}$ from the single crystal XRD refinement

Atom	Wyck.	Site	S.O.F.	x	y	z	U_{eq}
Ba1	12d	-4..		0.5	0.25	0	0.0122(2)
Ba2	8c	.3m		0.1759(1)	0.1759(1)	0.1759(1)	0.03039(17)
Fe1	2a	-43m		0	0	0	0.0081(4)
Fe2	24g	..m	0.56(3)	0.7101(1)	0.1010(1)	0.1010(1)	0.0132(3)
Zn1	24g	..m	0.44(3)	0.7101(1)	0.1010(1)	0.1010(1)	0.0132(3)
Si1	6b	-42.m		0.5	0	0	0.0084(8)
S2	12e	2.mm		0.1919(2)	0	0	0.0181(6)
S3	24g	..m		0.7285(1)	0.2715(1)	0.0667(2)	0.0257(7)
O1	24g	..m		0.4316(5)	-0.0715(3)	0.0715(3)	0.0124(12)

Table S3. Anisotropic Thermal Parameters Uij ($Å^2$) for $Ba_{10}Fe_{7.75}Zn_{5.25}S_{18}Si_3O_{12}$ from the single crystal XRD refinement

Atom	U_{11}	U_{22}	U_{33}	U_{12}	U_{13}	U_{23}
Ba1	0.0136(2)	0.0094(3)	0.0136(2)	0	0	0
Ba2	0.0304(3)	0.0304(3)	0.0304(3)	-0.0005(3)	-0.0005(3)	-0.0005(3)
Fe1	0.0081(7)	0.0081(7)	0.0081(7)	0	0	0
Fe2	0.0120(7)	0.0138(5)	0.0138(5)	-0.0009(3)	-0.0009(3)	0.0017(5)
Zn1	0.0120(7)	0.0138(5)	0.0138(5)	-0.0009(3)	-0.0009(3)	0.0017(5)
Si1	0.0102(19)	0.0076(11)	0.0076(1)	0	0	0
S2	0.0159(14)	0.0193(9)	0.0193(9)	0	0	0.0049(16)
S3	0.0154(8)	0.0154(8)	0.046(2)	-0.0019(9)	-0.0086(8)	0.0086(8)

Table S4. Main Distances (Å) for $Ba_{10}Fe_{7.75}Zn_{5.25}S_{18}Si_3O_{12}$ from the single crystal XRD refinement

Atom1	Atom2	d 1,2 [Å]
Ba1	Fe2	3.6905(10)*4
Ba1	Si1	3.33450(5) *2
Ba1	S3	3.189(2)*4
Ba1	O1	2.722(4)*4
Ba2	Fe1	4.0637(7)
Ba2	Fe2	4.1172 (11)*6
Ba2	S2	3.3248(7)*3
Ba2	S3	3.705(3)*3
Ba2	S3	3.574(3)*3
Fe1	S2	2.559(3)*6
Fe2	S2	2.3110(19)
Fe2	S3	2.332(2)*2
Fe2	O1	1.972(6)
Si1	O1	1.627(5)*4

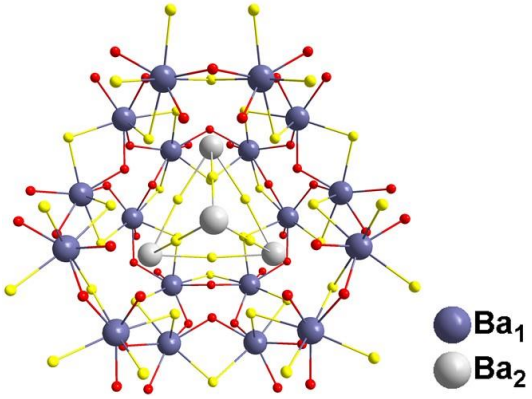

Figure S1. Ba1 and Ba2 sub-lattice, for clarity only Ba atoms and their environment (O, S) are represented. Ba atoms are placed in the voids of the structure that we describe and it the voids occupied by Ba2 are larger than the one occupied by Ba1, this might be at the origin of the larger thermal displacement observed for Ba2. More into details, Ba1 has a set of rather symmetric distances with four equal Ba-O distances of 2.722(4) Å and four equal Ba-S distances of 3.189(2) Å. On another hand Ba2 is involved in two sets of three Ba-S distances, i.e. 3.325(1) Å and 3.574(3) Å, (forming a trigonal prism) and in another set of three longer distances also delimiting this cavity and equal to 3.705(3) Å. The Ba2-S distances are in the highest part of the range expected for Ba-S bonds compared to those found for Ba1.

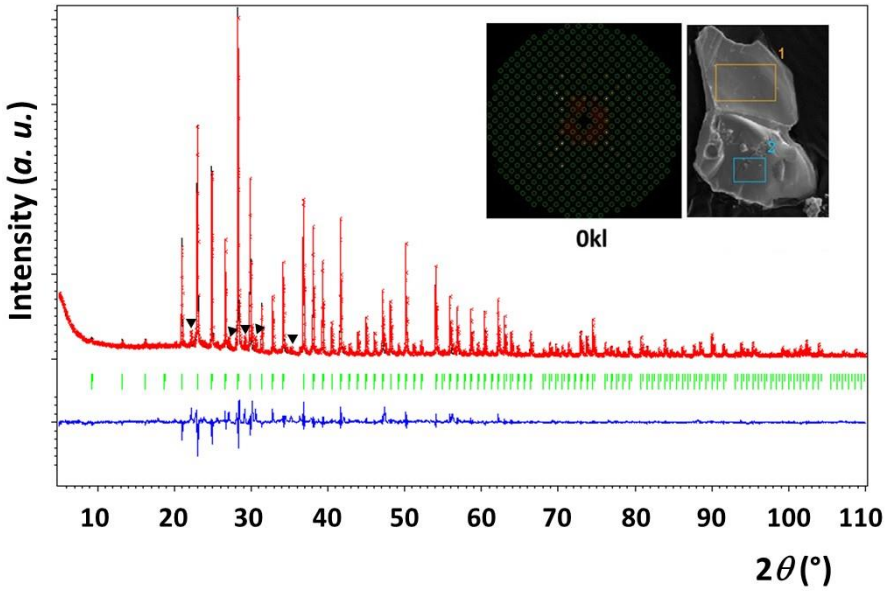

Figure S2. XRD Rietveld refinement of a powder of $Ba_{10}Fe_{7.75}Zn_{5.25}S_{18}Si_3O_{12}$. The experimental (red) and calculated (black) patterns are superimposed. The difference curve is represented in blue and the Bragg peaks positions in green. The most significant unindexed low intensity impurity peaks are pointed with black triangles. A SEM image of a single crystal and a precession image showing plane 0kl (single crystal XRD) are also shown as insets.

The XRD data was collected at room temperature using the Cu $K_{\alpha1}$ and Cu $K_{\alpha2}$ radiation ($\lambda \approx 1.54187$ Å) in the 2θ range 5 – 110° with a step size of 0.02° and an acquisition time of 1 second for each step. The profile and the cell parameters were refined with the Le Bail method. The background was fitted using a linear interpolation between a selection of points. A pseudo-Voigt function was used for the peak-shape model. Then the structure was refined using the Rietveld method[1] with the Program Jana2006[2]. The final Rietveld refinement converged with the cubic unit cell parameter a= 13.3350 (1) Å and the

reliability factors R_{obs}= 0.0323, wR_{obs}= 0.0384, R_{all}= 0.0328, wR_{all}= 0.0388 and a goodness of fit (GOF) of 3.29. We could refine the thermal parameters of the heaviest atoms as anisotropic (Ba1, Ba2 and Fe2), see Table S7. The mixed site Fe2/Zn2 and Si1, S1, S2 and O1 were refined as isotropic. The atomic parameters and isotropic thermal displacements are given in Table S6. The complementary occupation of the Fe2/Zn1 mixed site was also refined and it converged to 0.47(7)/0.53(7) for Fe/Zn. This is close to half/half occupancy as found from the single crystal refinement with 0.56(3)/0.44(3). The slight discrepancy can be expected from the powder data versus single crystal refinements regarding this particular mixed Fe/Zn site. In particular, from the powder only the heaviest atoms Ba1, Ba2 as well as Fe1 could be properly refined with anisotropic thermal displacement and not the mixed Fe/Zn site contrarily to the single crystal data. Overall, regarding the error on the powder ratio value (higher than the single crystal one), the ratio is consistent with the initial single crystal refinement. It is also consistent with the XPS and magnetic fit results that depend on the Fe content.

Finally, the structure refined by the Rietveld method from powder XRD is consistent with the single crystal XRD refinement. The cubic unit cell parameter *a* (13.3350(1) Å) is very close to the value found from the single crystal (a= 13.3380(1) Å).

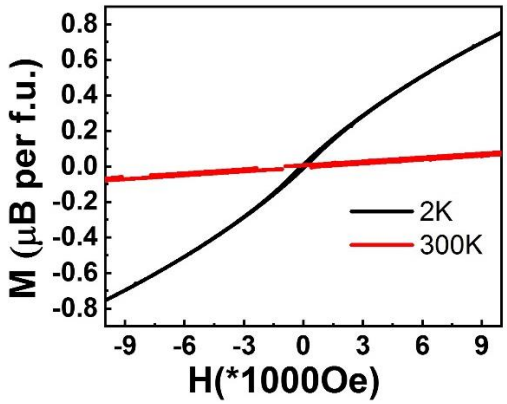

Figure S3. Field dependence of the magnetization at the constant temperatures of 2 and 300 K.

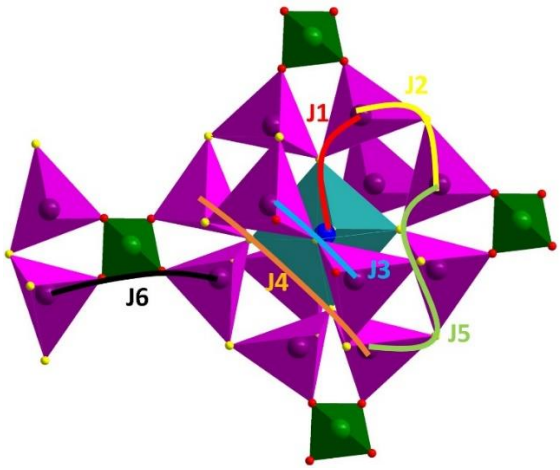

Figure S4. Magnetic paths in $Ba_{10}Fe_{7.75}Zn_{5.25}S_{18}Si_3O_{12}$.

Magnetic exchanges in $Ba_{10}Fe_{7.75}Zn_{5.25}S_{18}Si_3O_{12}$. The properties discussed above are coherent with the complex magnetic exchanges observed between iron ions. Six different magnetic paths (disturbed by Zn in the

real structure) involving the complex magnetic cluster extended in the three directions are presented below. The $Fe1^{2+}$ localized in the octahedral site is coupled to $Fe2^{3+}$ with one Fe1-S2-Fe2 super-exchange (SE) path (J1). Then intra-cluster Fe2 ions (tetrahedra) coupling occur with two SE (J2 and J3) and two super-super-exchanges (SSE) paths (J4 and J5) while inter-clusters happen trough SSE only (J6). The geometrical parameters associated with these exchange paths are summarized in Table S5 and represented in Figure S4. Intra-clusters magnetic interaction are mediated trough sulfide anions while inter-cluster SSE involve oxide anions.

From a local point of view and for all different J paths, multiple Fe-Fe interactions are possible because the tetrahedral mixed valence $Fe^{2+/3+}$ site is always involved: i) For J1, $Fe^{2+}_{(Oh)}$-$Fe^{3+}_{(Td)}$ or $Fe^{2+}_{(Oh)}$-$Fe^{2+}_{(Td)}$. ii) For J2-J6, $Fe^{2+}_{(Td)}$-$Fe^{3+}_{(Td)}$ or $Fe^{2+}_{(Td)}$-$Fe^{2+}_{(Td)}$ or $Fe^{3+}_{(Td)}$-$Fe^{3+}_{(Td)}$.

Table S5. Magnetic coupling with distances and angles of the super-exchanges (SE) and super-super exchanges (SSE) paths in $Ba_{10}Fe_{7.75}Zn_{5.25}Si_3S_{18}O_{12}$

	atom1	atom2	d[1,2] (Å)	(SE) Fe-S-Fe (Å)	(SSE) Fe-O…O-Fe (Å) or Fe-S…S-Fe	(SSE) O…O or S…S (Å)	Angles Fe-O-Fe (°) or Fe-S-Fe (°)
J1	Fe1	Fe2	4.310(1)	Fe1-S2=2.56(1) S2-Fe2=2.311(2)	-	-	Fe1-S2-Fe2=124.44(3)
J2	Fe2	Fe2	3.562(1)	Fe2-S3=2.332(2) S3-Fe2=2.332(2)			Fe1-S2-Fe2=99.586(82)
J3	Fe2	Fe2	3.811(1)	Fe2-S2=2.310(2)	-	-	Fe2-S2-Fe2 = 111.1(0)
J4	Fe2	Fe2	7.374(1)		Fe2-S2=2.311(2)	S2-S2=3.62(1)	Fe2-S2-S2=144.32(2)
J5	Fe2	Fe2	6.387(1)		Fe2-S2=2.311(2) S3-Fe2=2.332(2)	S2-S3=3.877(3)	Fe-S3-S2=82.9(1) Fe-S2-S3=121.58(3)
J6	Fe2	Fe2	6.22(1)	-	Fe2-O1= 1.971(7) O1-Fe2= 1.971(7)	O1-O1 = 2.64(1)	Fe-O1-O1=143.85(21)

Table S6. Powder XRD Rietveld refinement: Atomic Positions and Isotropic Thermal Displacement for $Ba_{10}Fe_{7.75}Zn_{5.25}S_{18}Si_3O_{12}$

Atom	Wyck.	Site	S.O.F.	x/a	y/b	z/c	U [Å²]
Ba1	12d	-4..		1/2	1/4	0	0.0092(9)
Ba2	8c	.3m		0.1755(2)	0.1755(2)	0.1755(2)	0.0278(7)
Fe1	2a	-43m		0	0	0	0.018(2)
Fe2	24g	..m	0.47	0.7111(3)	0.1006(3)	0.1006(3)	0.009(2)
Zn1	24g	..m	0.53	0.7111(3)	0.1006(3)	0.1006(3)	0.009(2)
Si1	6b	-42.m		1/2	0	0	0.002(3)
S2	12e	2.mm		0.1918(8)	0	0	0.007(3)
S3	24g	..m		0.7274(5)	0.2726(5)	0.0633(6)	0.021(3)
O1	24g	..m		0.433(1)	-0.0705(10)	0.0705(10)	0.011(6)

Table S7. Powder XRD Rietveld refinement: Anisotropic Thermal Displacement for $Ba_{10}Fe_{7.75}Zn_{5.25}S_{18}Si_3O_{12}$

Atom	U_{11}	U_{22}	U_{33}	U_{12}	U_{13}	U_{23}
Ba1	0.012(1)	0.004(2)	0.012(1)	0	0	0
Ba2	0.028(1)	0.028(1)	0.028(1)	-0.004(1)	-0.004(1)	-0.004(1)
Fe1	0.018(4)	0.018(4)	0.018(4)	0	0	0

Table S8. Vogel Fulcher parameters

$\omega_0/2\pi$	E_a (eV)	T_0 (K)
10^9	1.34×10^{-3}	2.21
10^{10}	1.86×10^{-3}	2.00
10^{11}	2.47×10^{-3}	1.78
10^{12}	3.16×10^{-3}	1.57
10^{13}	3.94×10^{-3}	1.36

1 A. W. Sleight, *Mater. Res. Bull.*, 1994, **29**, 695.

2 V. Petříček, M. Dušek and L. Palatinus, *Zeitschrift für Krist. - Cryst. Mater.*, 2014, **229**, 345–352.